THE JOURNAL OF BIOLOGICAL CHEMISTRY Vol. 277, No. 44, Issue of November 1, pp. 42017–42027, 2002
Printed in U.S.A.

Oxidative Modification of Aldose Reductase Induced by Copper Ion

DEFINITION OF THE METAL-PROTEIN INTERACTION MECHANISM*

Received for publication, July 11, 2002, and in revised form, August 12, 2002
Published, JBC Papers in Press, August 14, 2002, DOI 10.1074/jbc.M206945200

Ilaria Cecconi, Andrea Scaloni‡, Giulio Rastelli§, Maria Moroni, Pier Giuseppe Vilardo, Luca Costantino§, Mario Cappiello, Donita Garland¶, Deborah Carper¶, J. Mark Petrash‖, Antonella Del Corso, and Umberto Mura**

From the Dipartimento di Fisiologia e Biochimica, Università di Pisa, via S. Maria, 55, 56100 Pisa, Italy, the ‡Proteomics and Mass Spectrometry Laboratory, I.A.B.B.A.M., National Research Council, 80147 Napoli, Italy, the §Dipartimento di Scienze Farmaceutiche, Università di Modena e Reggio Emilia, 41100 Modena, Italy, the ¶National Eye Institute, National Institutes of Health, Bethesda, Maryland 20892, and the ‖Departments of Ophthalmology and Visual Sciences and of Genetics, Washington University School of Medicine, St. Louis, Missouri 63110

Aldose reductase (ALR2) is susceptible to oxidative inactivation by copper ion. The mechanism underlying the reversible modification of ALR2 was studied by mass spectrometry, circular dichroism, and molecular modeling approaches on the enzyme purified from bovine lens and on wild type and mutant recombinant forms of the human placental and rat lens ALR2. Two equivalents of copper ion were required to inactivate ALR2: one remained weakly bound to the oxidized protein whereas the other was strongly retained by the inactive enzyme. Cys^{303} appeared to be the essential residue for enzyme inactivation, because the human C303S mutant was the only enzyme form tested that was not inactivated by copper treatment. The final products of human and bovine ALR2 oxidation contained the intramolecular disulfide bond Cys^{298}-Cys^{303}. However, a Cys^{80}-Cys^{303} disulfide could also be formed. Evidence for an intramolecular rearrangement of the Cys^{80}-Cys^{303} disulfide to the more stable product Cys^{298}-Cys^{303} is provided. Molecular modeling of the holoenzyme supports the observed copper sequestration as well as the generation of the Cys^{80}-Cys^{303} disulfide. However, no evidence of conditions favoring the formation of the Cys^{298}-Cys^{303} disulfide was observed. Our proposal is that the generation of the Cys^{298}-Cys^{303} disulfide, either directly or by rearrangement of the Cys^{80}-Cys^{303} disulfide, may be induced by the release of the cofactor from ALR2 undergoing oxidation. The occurrence of a less interactive site for the cofactor would also provide the rationale for the lack of activity of the disulfide enzyme forms.

Transition metals have a relevant role among systems that can induce or modulate oxidative stress. They are both able to promote the formation of reactive oxygen species (1) and to act as cofactors in enzymatic systems devoted to counteract oxidative stress. The important role of the copper ion as an effective prosthetic group for special protein functions and its role as a potential toxic agent in cell function are handled by the cell through a fine control of the free copper level by highly efficient metal chelating proteins (2, 3). In this regard, it is worth noting the extensive cell damage associated with pathologies resulting from both excess and a deficit of copper, such as Wilson's and Menkes's disease, respectively (4, 5).

When the concentration of free copper increases, either by environmental or pathological causes, cell damage likely occurs (6–10). The effectiveness of copper ion in inducing protein as well as nucleic acid oxidation, by eliciting the generation of reactive oxygen species through a Fenton-type reaction, is well documented (11–16). Moreover, because of its ability to bind proteins and nucleic acids, copper has the potential to specifically promote *in situ* oxidative modification reactions. Thus, it is important to define the mechanisms underlying processes induced by copper-protein interaction.

The effect of the copper ion on aldose reductase (alditol: $NADP^+$ oxidoreductase, EC 1.1.1.21) (ALR2),[1] isolated from bovine lens was previously described (17). It appears that the enzyme, which was previously shown to be especially susceptible to thiol-mediated oxidation (18–22), is highly sensitive to Cu(II). The enzyme is readily inactivated by the metal ion through an oxygen independent modification process. The modified enzyme, fully reactivated in the presence of dithiothreitol, was postulated to contain an intramolecular disulfide bond and to carry two equivalents of bound copper ion. Based on the characterization of the inactivation process and on the measurement of the redox state of the bound copper on the enzyme, it was concluded that the metal ion responsible for ALR2 inactivation was directly involved in a site specific oxidation mechanism of the enzyme.

In this paper, the rationale for the definition of the copper binding site(s) and the formation of the disulfide bond in ALR2 is put forward through mass spectrometry, circular dichroism, and molecular modeling approaches on the enzyme and its mutants from different species.

EXPERIMENTAL PROCEDURES

Materials

NADPH, D,L-glyceraldehyde, dithiothreitol, GSH, EDTA, endoproteinase Lys-C, iodoacetamide, DTT, and myoglobin were purchased from Sigma. Bathocuproinedisulfonic acid was from Jannsen Pharma-

* This work was supported in part by grants from the Italian Board for Education, University and Research (MIUR), Pisa University, and the National Research Council. The costs of publication of this article were defrayed in part by the payment of page charges. This article must therefore be hereby marked "*advertisement*" in accordance with 18 U.S.C. Section 1734 solely to indicate this fact.

** To whom correspondence should be addressed: Dept. di Fisiologia e Biochimica, via S. Maria, 55, 56100 Pisa, Italy. Tel.: 39-050-500292; Fax: 39-050-502583; E-mail: umura@dfb.unipi.it.

[1] The abbreviations used are: ALR2, aldose reductase; b-ALR2, bovine lens ALR2; h-ALR2, human placental recombinant ALR2; h-C298S, h-C80S, h-C303S, cysteine to serine mutated h-ALR2; r-ALR2, rat lens recombinant ALR2; r-C298S, cysteine to serine mutated r-ALR2; CAM, carboxamidomethyl; DTT, dithiothreitol; GS-ALR2, glutathione-modified ALR2; LC-ESIMS, liquid chromatography-electrospray ionization mass spectrometry; 2-ME, 2-mercaptoethanol; MD, molecular dynamics; MM, molecular mechanics.

ceutical. All electrophoresis reagents and isoelectric focusing standards were from Bio-Rad. Ampholine PAG plates, pH 4.0–6.5, for isoelectric focusing were from Amersham Biosciences. Copper(II) chloride and all inorganic chemicals were of reagent grade and were from BDH. The ALR2 inhibitor (S)(+)-6-fluoro-2,3-dihydrospiro[4H-1-benzopyran-4,4′-imidazolidine]-2′,5′-dione (Sorbinil) (23) was a gift from Dr. G. Caccia, Laboratori Baldacci S.p.A., Pisa, Italy. The complex (bathocuproinedisulfonic acid)$_2$Cu(I) was a gift from Dr. R. L. Levine, Laboratory of Biochemistry, NHLBI, National Institutes of Health, Bethesda, MD. γ-Glutamyl-cysteinyl-2-[^{3}H]glycine ([^{3}H]GSH), 1 Ci/mol was purchased from PerkinElmer Life Sciences.

Generation of Mutated Enzymes and Enzyme Purification

The purification of b-ALR2 was performed as previously described (24). The pure native enzyme (specific activity 1.12 units/mg) was stored at 4 °C in 10 mM sodium phosphate buffer, pH 7.0 (S-buffer), supplemented with 2 mM DTT.

Expression of h-ALR2 in *Escherichia coli* was done as previously described (25). Recombinant aldose reductase was extracted from host cells by osmotic shock and stored at −70 °C until used. Wild type and mutated forms of h-ALR2 were purified to electrophoretic homogeneity by the same chromatographic steps used for the bovine lens enzyme (24); the pure enzymes were stored at 4 °C in S-buffer supplemented with 2 mM DTT. The specific activities of h-ALR2 and its C298S, C80S, and C303S mutants were 3.9, 9.8, 3.1, and 6.2 units/mg, respectively.

E. coli expressing r-ALR2 and its mutants was grown as previously described (26). The cells were washed twice in 20 mM imidazole buffer, pH 7.2, and centrifuged. The cell pellet was resuspended in 10 ml of the same buffer, sonicated, and stored at −70 °C until used. r-ALR2 and its mutants were purified to electrophoretic homogeneity by the same chromatographic steps used for the bovine lens enzyme (24); the pure enzymes were stored at 4 °C in S-buffer supplemented with 2 mM DTT. The specific activities of r-ALR2 and its H200Q, H110Q, H41Q, H187Q, and C298S mutants were 4.5, 5.2, 0.6, 4.0, 4.0, and 5.2 units/mg, respectively.

Measurement of Enzyme Activity

The ALR2 activity and sensitivity to inhibition by Sorbinil were measured as previously described by using D,L-glyceraldehyde as substrate (17).

Enzyme Inactivation

Before use, the enzyme forms were extensively dialyzed against S-buffer. If not otherwise specified, copper treatment of h-ALR2 forms was performed by supplementing the enzyme after dialysis with a stoichiometric amount of $NADP^+$. When r-ALR2 was used, 30 μM DTT was present in the dialysis buffer and 4 μM DTT was constantly present in all further incubations.

All tested enzyme forms, from 3 to 8 μM final concentrations, were incubated for the proper time at 25 °C in S-buffer supplemented with $CuCl_2$ to give final ratios of [Cu(II)]/[enzyme] from 0.5 to 5, as specifically indicated. At the end of the incubation, 0.5 mM EDTA was added and the enzyme activity was measured. To detect copper bound to ALR2, the samples were extensively dialyzed at 4 °C against S-buffer containing 0.5 mM EDTA.

Measurement of Copper

The concentration of Cu(I) was determined by a complexometric method as previously described (17) by measuring the formation of the complex between the metal ion and bathocuproinedisulfonic acid.

Circular Dichroism Analysis

Circular dichroism spectra were obtained on a Jasco J40AS spectropolarimeter with a cylindrical 10-mm path length cuvette kept at 10 °C. A spectral bandwidth of 2 nm was used.

Alkylation of Aldose Reductase Samples with Iodoacetamide

To block reduced cysteines, ALR2 samples were alkylated with 1.1 M iodoacetamide in 0.25 M Tris-HCl, 1.25 mM EDTA, containing 6 M guanidinium chloride, pH 7.0, at room temperature for 1 min in the dark. Proteins were freed from salt and reagent excess by passing the reaction mixture through an analytical Vydac C_4 column as previously reported (22). Protein samples were manually collected and lyophilized.

ESIMS Analysis

Electrospray mass spectra of intact protein species were recorded by using an API-100 single quadrupole mass spectrometer (Applied Biosystems) equipped with an atmospheric pressure ionization source as previously reported (22). Mass calibration was performed by means of the multiply charged ions from a separate injection of horse heart myoglobin (molecular mass 16,951.5 Da). All masses are reported as average values.

Enzymatic Hydrolysis

Samples of carboxamidomethylated aldose reductase (150 μg) were digested with endoproteinase Lys-C in 0.4% ammonium bicarbonate, pH 8.0, at 37 °C overnight, using an enzyme/substrate ratio of 1:100 (w/w).

LC-ESIMS Analysis

ALR2 digests were analyzed using a LCQ Deca mass spectrometer (ThermoFinnigan) equipped with an electrospray source connected to a HP1100 chromatographic system (Agilent, Palo Alto, CA). Peptide mixtures were separated on a narrow bore Vydac C_{18} column (The Separation Group) using a linear gradient from 5 to 70% acetonitrile containing 0.1% trifluoroacetic acid, over a period of 65 min, at a flow rate of 0.2 ml/min. The column effluent was split 1:1 into the mass spectrometer connected on-line. The remaining part was spectrophotometrically detected at 220 nm. In the last case, peptides were manually collected and lyophilized for further characterization. Spectra were acquired in the range m/z 250–2000. Data were elaborated using the Excalibur software provided by the manufacturer. The instrument was calibrated using a mixture of caffeine, MRFA peptide, and Ultramark 1621.

A determination of the relative abundance of the peptides containing Cys^{80}, Cys^{298}, and Cys^{303} was performed as previously reported by Vinci *et al.* (27). Briefly, because different peptides containing a specific Cys residue could exist, the ion current for peptides containing a specific Cys residue (in reduced or oxidized form) was obtained by summing the ion current relative to all peptides containing that cysteine (in reduced or oxidized form). To obtain the relative abundance of a specific cysteine in reduced or oxidized form, this value was divided by the ion current produced by all peptides containing Cys^{80}, Cys^{298}, and Cys^{303}. Because different peptides may ionize with different efficiencies, it was not possible to evaluate the absolute abundance of each reduced or oxidized cysteine. It was, nevertheless, possible to compare the trends in the oxidation of the different cysteine residues.

Protein Sequence Analysis

Automated N-terminal degradation of the purified peptides was performed by using Procise 491 protein sequencer (Applied Biosystems) equipped with a 140C microgradient apparatus and a 785A UV detector (Applied Biosystems) for the automated identification of phenylthiohydantoin-derivative.

Other Methods

Protein concentration was determined according to Bradford (28) using bovine serum albumin as the standard. Electrophoretic and isoelectrofocusing analyses were performed as previously described (17). Radioactivity measurements were done using a Beckman LS5000CE scintillation counter and Optiphase Hi Safe as scintillation fluid with a counting efficiency of 50% as determined by the tritium standard quench curve of the instrument.

Molecular Modeling

Molecular mechanics and molecular dynamics simulations were performed with the sander_classic module of AMBER6 (29), using the Cornell *et al.* (30) force field. Calculations were performed on a IBM-SP3 computer. Graphical display and manipulations were performed on Silicon Graphics O2 workstations using MIDAS (31).

Force Field Parameters of Copper—Force field parameters for copper(II) have been developed in the present work and tested on plastocyanin. An ionic (nonbonded) approach (32) was adopted in modeling the metal. The van der Waals R^* of copper(II) was interpolated from a linear plot of the R^* values of the metal ions contained in the AMBER force field against their atomic radii (33); similarly, the well depth ϵ was interpolated from an exponential plot of the ϵ values of the same metal ions *versus* their atomic radii. Values of $R^* = 1.26$ Å and $\epsilon = 0.0123$ kcal/mol were obtained.

The coordination geometry of copper extracted from the crystal structure of plastocyanin (34) was used for charge calculations of copper; to this aim, the Cα carbons of the four amino acids coordinating copper (His^{37}, His^{87}, Cys^{84}, and Met^{92}) were truncated with methyl groups, and cysteine was modeled as anionic (35, 36). The atomic charge of Cu(II) was obtained from an electrostatic potential fit to STO-3G and 6–31G*

ab initio wave functions, using GAUSSIAN94 (37), followed by standard RESP fit (38, 39). In the first case, a STO-3G basis set for copper and the whole coordination sphere was used, whereas a mixed 6–31G* basis set for the amino acids and a STO-3G basis set for copper was used in a second case. Atomic charges of copper of +0.71 and +1.13 were obtained, respectively. In both cases, the formal +2 charge of copper turned out to be significantly reduced upon coordination. As plastocyanin might not be an appropriate model for the copper coordination in ALR2, which is unknown, charge calculations were repeated for a system comprised of copper and six coordinating water molecules, using STO-3G. We still found that the charge of copper reduces to +1.08, a finding that confirms that the charge of the metal has to be reduced from +2 in liquid simulations, regardless of the nature of the residues that coordinate the metal.

To test the reliability of the present R^*, ϵ, and charge parameters of copper, MM and MD calculations were performed on the whole plastocyanin molecule using AMBER. Hydrogens were added to the protein and then optimized, keeping the heavy atoms of the protein fixed at their original positions. Counterions were placed around the charged residues at the surface of the protein to neutralize the system. The parameters for Na^+ and Cl^- were taken from the works of Åqvist (40) and Jorgensen (41), respectively. Crystallographic water molecules buried inside the protein were maintained and a 15-Å spherical cap of TIP3P (42) water molecules centered on copper was added, resulting in 83 additional waters.

Three independent MM and MD simulations were performed by setting the charge on copper at +2 (formal charge), +1.13 (mixed 6–31G*/STO-3G), and +0.71 (ST0–3G). In each case, 3,000 steps of conjugate-gradient minimization with MM were performed on the water molecules first, followed by 10,000 steps minimization of the protein residues at 12-Å distance from copper and all the water molecules. A 10-Å cut-off for the nonbonded interactions was adopted. Molecular dynamics was performed for 100 ps at 27 °C, using SHAKE (43) to constrain bond lengths at their equilibrium values. Coordinates were collected every 0.1 ps for analysis, with the last 20 ps averaged for analysis. The root mean square deviations between the averaged structures and the crystal structure of plastocyanin (34) have been analyzed. Taking into account the root mean square deviation values corresponding to the backbone atoms of the protein, values of 0.50, 0.36, and 0.28 were obtained for the simulations employing the +2, +1.13, and +0.71 charge on copper, respectively. Root mean square deviations limited to the coordination sphere of copper (*i.e.* copper, His^{37}, His^{87}, Cys^{84}, and Met^{92}) gave a similar trend (0.47, 0.28, and 0.20 for the three simulations). Therefore, MD with the formal charge of +2 on copper gave the worst results both in terms of reproducing the crystal structure of plastocyanin and the coordination geometry of copper. In contrast, the +0.71 simulation gave the best results and this charge was used throughout for the aldose reductase simulations.

Noncovalent Interactions between ALR2 and Copper—As it will be shown, an *ad hoc* strategy was devised to simulate the modification of ALR2 as a two-step process in which copper initially forms a noncovalent complex with ALR2 and, subsequently, induces the disulfide bridge formation.

Two copper ions were docked into the structure of the human ALR2 holoenzyme (44). Because Cys^{80}, Cys^{298}, and Cys^{303} are the three cysteines involved in the formation of a disulfide bridge, copper ions were initially positioned to interact with these residues. One copper ion was positioned close to Cys^{80} and one close to Cys^{303} to investigate the formation of the Cys^{80}-Cys^{303} disulfide, and one copper ion was positioned close to Cys^{298} and one close to Cys^{303} for the Cys^{298}-Cys^{303} disulfide. When coordinating copper, cysteines were assigned a deprotonated form (35, 36). The ALR2 structures have been prepared using a procedure similar to that described for plastocyanin, with hydrogens added and counterions placed. The parameters for the cofactor were taken from previous work. Structures were solvated with spherical caps of more than 2000 TIP3P (42) water molecules centered on the center of mass of ALR2.

The following protocol was adopted for minimization and dynamics. A few steps of minimization with MM were performed on the two copper ions keeping the protein fixed at its original position to adjust their initial position with respect to the two cysteines. Prior to energy minimization of ALR2, only the water molecules were energy minimized and then subjected to 50 ps of MD at 27 °C to let the solvent equilibrate around the solute. Then, 5000 steps of minimization were performed on the whole system. 300 ps of MD at 27 °C was then performed starting from the minimized structure, using the same conditions described for plastocyanin. The whole structure was allowed to move during MD. MD was continued for over 800 ps in the case of the enzyme loaded with the two copper ions close to Cys^{298} and Cys^{303}.

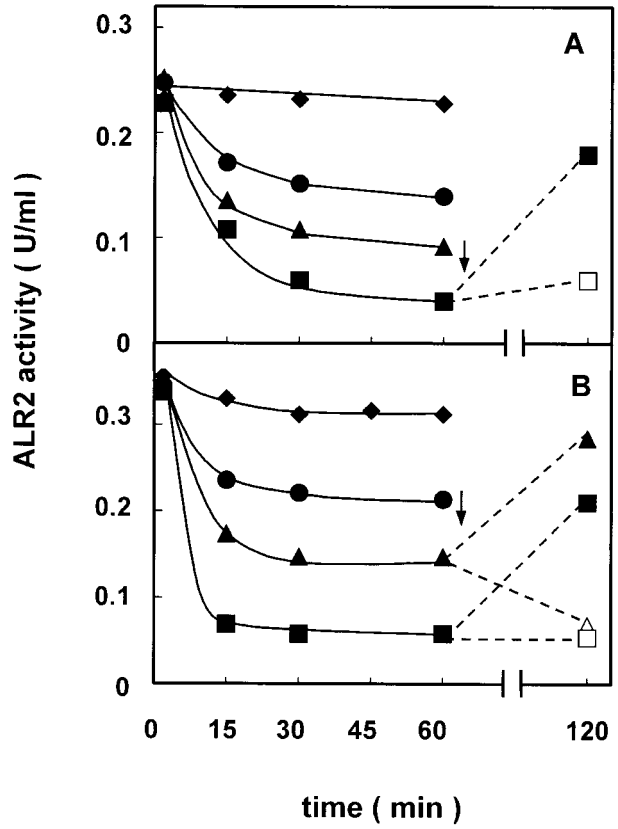

FIG. 1. **Inactivation of human and rat aldose reductase induced by copper ion.** ALR2 at the final concentration of 3.5 μM was incubated at 25 °C both in the absence (♦) and presence of the following $CuCl_2$ μM concentrations: 1.75 (●), 3.5 (▲, Δ), 7.0 (■, □). The incubations were performed either in S-buffer for h-ALR2 (*panel A*) or in S-buffer containing 4 μM DTT for r-ALR2 (*panel B*). At the times indicated by the *arrows*, 3 mM DTT was added and the mixtures were again incubated at 25 °C (*dashed lines*). *Closed* and *open symbols* refer to the enzyme activity measured in the absence and presence of 10 μM Sorbinil, respectively.

Disulfide Bond Formation—Because the sulfur atoms of Cys^{80} and Cys^{303}, after the 300 ps MD with copper, turned out to be much closer than the corresponding atoms in the crystal structure of the holoenzyme, the last minimized structure obtained from the noncovalent simulation described in the force field parameter section was used as the starting point for building a covalent disulfide bond between these cysteines. Five thousand steps of minimization and 800 ps of MD at 27 °C were performed on the enzyme carrying the Cys^{80}-Cys^{303} disulfide with coordinates collected for the subsequent analysis.

Because, after 800 ps of MD, Cys^{298} and Cys^{303} were not sufficiently close to form a disulfide in the noncovalent complexes, a different strategy was used to build a model structure carrying this disulfide. Using the homology modeling software Model er6 (45), the sequence of ALR2 was artificially aligned with itself, with the only difference being that while the template did not contain any disulfide (the crystal structure of the holoenzyme), a disulfide was explicitly requested in the modeled structure. This approach produced an initial structure of ALR2 carrying the disulfide; the quality of the structure was evaluated using PROCHECK (46). Then, the two copper ions were docked close to Cys^{298} and Cys^{303}, and the structure was refined with MM and MD using the same protocol described above. 5000 steps of minimization were performed, and the structure was equilibrated with 900 ps of MD.

RESULTS

Copper-dependent Inactivation of Human and Rat Recombinant ALR2—The recombinant h-ALR2 and r-ALR2 were readily inactivated by low concentrations of Cu(II) (Fig. 1). The rate and extent of inactivation were dependent on copper ion concentration. Moreover, in both cases enzyme activity was recovered upon addition of DTT. Following incubation with

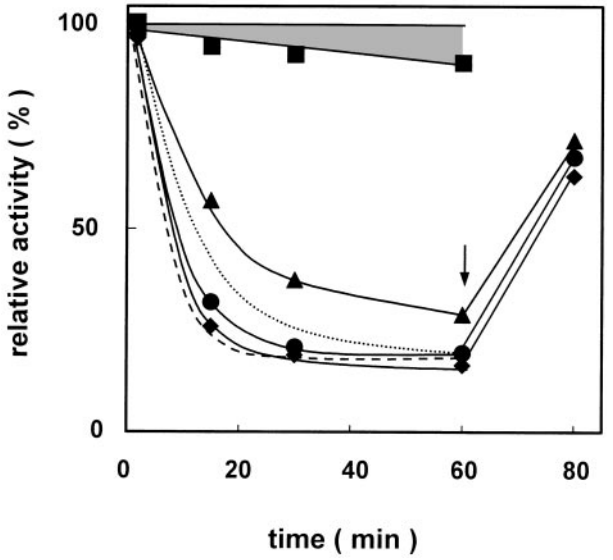

FIG. 2. **Effect of copper ion on human and rat Cys mutant recombinant ALR2 enzymes.** Human C298S (●), C80S (▲), and C303S (■), and rat C298S (♦) ALR2 mutated enzymes, were incubated at the final concentration of 3.5 μM at 25 °C in the presence of 7 μM $CuCl_2$ and enzyme activity was measured. At the time indicated by the *arrow*, 3 mM DTT was added and the mixtures were incubated again at 25 °C. *Dashed* and *dotted lines* refer to human and rat wild type, respectively, incubated as above in the presence of $CuCl_2$ (data taken from Fig. 1*A* and *B*). The *shaded area* refers to the activity of the different enzymes incubated in the absence of $CuCl_2$.

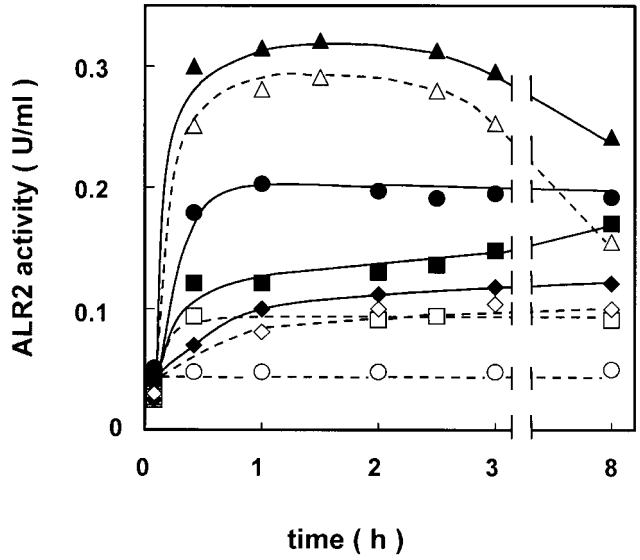

FIG. 3. **Effect of thiol reducing conditions on copper-modified bovine lens ALR2.** Following $CuCl_2$ treatment for 90 min at 25 °C (at a [Cu(II)]/[enzyme] ratio of 2:1) and extensive dialysis against S-buffer supplemented with 0.5 mM EDTA, b-ALR2 at the final concentration of 5.3 μM was incubated at 25 °C in S-buffer in the presence of 3 mM of the following thiol compounds: DTT (●, ○), 2-ME (▲, Δ), GSH (■, □), cysteine (▼, ▽). *Closed* and *open symbols* refer to the enzyme activity measured in the absence and presence of 10 μM Sorbinil, respectively.

$CuCl_2$ and extensive dialysis at 4 °C against EDTA, r-ALR2 and h-ALR2 contained 1.8 ± 0.1 and 2.1 ± 0.1 equivalents of total metal ion per enzyme mole, respectively. This is consistent with that reported for the b-ALR2 (17). Moreover, EDTA or *o*-phenanthroline (1 mM), when initially present or when added at different times in the Cu(II)/ALR2 incubations mixtures, was able to prevent or block the enzyme modification (data not shown).

Some distinct differences were observed among the bovine, rat, and human enzymes. The rat lens enzyme, possibly because of the presence of an extra cysteine residue with respect to the human and bovine enzymes (47), is not stable unless low DTT concentrations (in the micromolar range) are present. On the other hand, h-ALR2, because of its reduced ability to retain the bound cofactor with respect to b-ALR2,[2] requires supplementation with $NADP^+$, which is always present during enzyme manipulation and incubation at a concentration ratio of [$NADP^+$]/[enzyme] of 1:1. Despite species-specific differences in the amino acid sequence among these enzymes, the high sequence homology can be ascribed as the reason for the substantially identical behavior of these enzymes with respect to copper-induced inactivation. Rat and human enzymes, mutated at different Cys residues (Fig. 2), as well as the rat enzyme mutated at several His residues (data not shown), are also inactivated by copper and their activities could be rescued by DTT treatment. The h-C298S and r-C298S enzymes were as sensitive to inactivation by copper as their respective wild type enzymes (Fig. 2). The h-C80S enzyme was slightly less susceptible to copper-induced inactivation than the native enzyme, but was still reactivated by DTT.

The h-C303S enzyme was insensitive to copper treatment; this enzyme retained 90% of the initial activity after 90 min of incubation in the presence of copper ion at a ratio of [Cu(II)]/[ALR2] of 2 (Fig. 2). A significant loss of enzyme activity was observed only when the concentration of copper was raised to [Cu(II)]/[ALR2] ratios higher than 3. However, under these conditions enzyme inactivation paralleled protein aggregation and enzyme activity was not recovered with DTT treatment (data not shown). The h-C303S enzyme also differed from wild type and other human mutated forms in the content of bound copper after treatment with the metal ion. Only 1.0 ± 0.1 eq of total copper ion per enzyme mole was detected on Cu(II)-treated, but still active, h-C303S. The h-C303S enzyme became sensitive to copper only when the pyridine cofactor, normally supplemented in the incubating mixtures of human enzymes, was omitted. However, under these conditions the activity of the h-C303S enzyme was recovered by incubation for 3 h at 37 °C with 0.5 mM EDTA. This was the only case among all of the ALR2 enzyme forms tested in which the inactivation could be reversed without addition of DTT. Thus, it appeared that Cys^{303} was the most relevant residue for the copper-induced inactivation of ALR2. The susceptibility to inactivation by copper was tested for a series of His mutants of r-ALR2 (*i.e.* H200Q, H110Q, H41Q, H187Q); in all cases at ratios of [Cu(II)]/[enzyme] of 3, the mutated enzymes were inactivated and the activity was recovered upon treatment with DTT (data not shown).

Effect of Thiol Compounds on the Copper-modified ALR2—DTT was able to rescue aldose reductase activity from Cu(II)-inactivated r-ALR2 and h-ALR2 (Fig. 1) as previously shown for the bovine lens enzyme (17). In fact, treatment with this reducing agent generated enzyme forms with a specific activity and sensitivity to inhibition by Sorbinil comparable with those of the respective native enzymes. GSH and 2-ME allowed a recovery of the enzyme activity, which was consistent with the generation of enzyme forms carrying the specific thiol reagent linked to the protein by a mixed disulfide bond. This conclusion was drawn from the results obtained with both b-ALR2 and h-ALR2 which, after inactivation by copper ion and removal of excess metal ion by extensive dialysis against EDTA, were treated at 37 °C with different reducing thiol compounds. In particular, for b-ALR2 (Fig. 3) 2-ME caused an increase of the activity ~2-fold that expected for the native ALR2, and the enzyme was scarcely affected by Sorbinil. These properties are

[2] I. Cecconi, unpublished observations.

TABLE I

LC-ESIMS analysis of native and Cu(II)-treated b-ALR2, h-ALR2, and human C298S mutant digests

Protein samples were alkylated under denaturing conditions prior to enzyme endoproteinase Lys-C digestion. $CAM_{1/2}$ indicated mono- and dicarboxamidomethylated species for the h-ALR2 C298S mutant and b- or h-ALR2, respectively.

Time	b-ALR2	Cu(II)-treated b-ALR2	h-ALR2	Cu(II)-treated h-ALR2	h-C298S	Cu(II)-treated h-C298S	Peptide
min				*Mass (Da)*			
4.5	562.3 ± 0.5	562.4 ± 0.4	563.3 ± 0.7	562.1 ± 0.5	563.3 ± 0.7	562.1 ± 0.5	(90–94)-CAM
10.2	1018.3 ± 0.6	1018.7 ± 0.4	960.1 ± 0.8	959.7 ± 0.9	960.4 ± 0.7	960.7 ± 0.3	(86–94)-CAM
14.7	1025.6 ± 0.9	1025.7 ± 0.8	1040.1 ± 0.7	1039.9 ± 0.5	1040.5 ± 0.4	1039.7 ± 0.3	(195–202)-CAM
26.9	1122.6 ± 0.6	1121.7 ± 0.6	1136.6 ± 0.5	1137.1 ± 0.4	1136.3 ± 0.9	1136.5 ± 0.8[a]	(78–85)-CAM
33.0	2218.8 ± 0.8	2217.9 ± 0.5	2218.5 ± 0.5	2217.9 ± 0.5	2218.1 ± 0.7	2217.4 ± 0.3	(177–194)-CAM
37.4	3297.5 ± 0.9	3297.2 ± 0.8	3327.7 ± 0.7	3327.5 ± 0.8	3327.4 ± 0.9	3327.3 ± 0.7	(33–61)-CAM
38.0	3035.3 ± 1.0	3035.9 ± 0.8	3091.3 ± 1.0	3091.9 ± 0.8	3091.6 ± 1.1	3091.5 ± 0.9	(62–85)-CAM
40.2	4091.5 ± 0.9	4091.8 ± 0.7[a]					(283–315)-CAM_2
40.9		3975.6 ± 1.3					(283–315)-S-S
42.3			3980.7 ± 0.9	3980.5 ± 1.2[a]	3908.4 ± 0.7		(275–307)-$CAM_{1/2}$
43.0				3864.9 ± 0.8			(275–307)-S-S
46.4			5045.9 ± 1.1	5046.3 ± 1.3[a]	4972.7 ± 0.8	4972.5 ± 1.1[a]	(275–315)-$CAM_{1/2}$
47.3				4929.7 ± 0.6			(275–315)-S-S
50.5		6341.7 ± 0.7		6302.0 ± 1.0			(263–315)-S-S
51.7	6457.9 ± 0.9	6457.7 ± 1.4[a]	6418.3 ± 1.3	6418.9 ± 1.1[a]	6345.7 ± 1.4	6345.4 ± 1.5[a]	(263–315)-$CAM_{1/2}$
53.9						5992.7 ± 0.9	(78–85)+(275–315)-S-S
						7365.2 ± 1.5	(78–85)+(263–315)-S-S

[a] Traces.

all comparable with those of a previously characterized 2-ME-modified ALR2 form (18, 48). GSH treatment of the copper-modified b-ALR2 induced a progressive recovery of enzyme activity and susceptibility to Sorbinil inhibition that was compatible with the formation of native ALR2. However, in this case, during the GSH-dependent reactivation process, the generation of GS-ALR2, an intermediate enzyme form, was observed. In fact, an enzyme form that did not bind the Matrex Orange A resin, and was not sensitive to Sorbinil (49), was detectable (data not shown). Finally, cysteine appeared to be a poor reducing agent of the oxidized enzyme, inducing a very modest recovery of ALR2 activity without a parallel recovery of the susceptibility to Sorbinil inhibition.

Concerning the human enzyme (data not shown), the activity of the Cu(II)-inactivated ALR2 was rescued by thiol compounds in a slightly different fashion than observed for the bovine enzyme. In this case, GSH was unable to induce a full reduction of the inactivated enzyme. Instead, GS-ALR2, in which Cys^{298} was previously shown to be involved in the formation of the mixed disulfide bond (19), is the only product of the reaction. In fact, after GSH treatment of the Cu(II)-inactivated h-ALR2, only one protein band in isoelectric focusing analysis (pI 5.9) was detectable; this enzyme form was insensitive to Sorbinil and did not bind the Matrex Orange A. When [^{3}H]GSH was used to recover enzyme activity from the Cu(II)-modified h-C80S enzyme, an incorporation of radioactivity consistent with the insertion of 1 (0.82 ± 0.02) glutathionyl residue per enzyme mole was observed. A further support of the involvement of Cys^{298} in the modification of the cysteine redox state of the enzyme subjected to copper treatment comes from the effect of the metal ion on the h-C298S enzyme. As shown above (Fig. 2) this form was readily inactivated by Cu(II), and the enzyme activity was fully recovered upon treatment with DTT. In the case of h-C80S and h-C298S enzymes, GSH and 2-ME were largely ineffective, allowing recoveries of only 30–40% of the expected enzyme activity value (data not shown).

Structural Analysis of Bovine and Human ALR2 and Their Products following Cu(II) Treatment—The amino acid sequences of b-ALR2, h-ALR2, and the h-C298S mutant were verified by ESIMS; the measured masses were 35,961.8 ± 3.4 Da, 35,721.3 ± 3.1 Da, and 35,704.9 ± 3.9 Da, respectively, in perfect agreement with the theoretical values (35,961.2, 35,722.5, and 35,706.2 Da, respectively).

b-ALR2 and h-ALR2 (3.5 μM) were incubated in S-buffer either in the absence or presence of 7 μM $CuCl_2$ for 180 min, quickly alkylated, and then analyzed by ESIMS as described under "Experimental Procedures." In the case of untreated b-ALR2 and h-ALR2, the spectra showed a single component at 36,360.9 ± 2.9 Da and 36,120.8 ± 3.2 Da, respectively, corresponding to a protein species containing seven carboxamidomethyl groups (theoretical values 36,360.5 Da and 36,121.5 Da). These results were consistent with the expected fully reduced form for both ALR2 species and demonstrated that the alkylation reaction went to completion. Similarly, the spectra of Cu(II)-treated b-ALR2 and h-ALR2 showed, in both cases, a main component at 36,244.9 ± 2.5 and 36,005.8 ± 2.7 Da, respectively, corresponding to an ALR2 form containing an intramolecular disulfide bond and five carboxamidomethyl groups (theoretical values 36,244.4 and 36,005.5 Da, respectively), with traces of fully reduced species.

To identify the amino acids involved in the intramolecular disulfide bond observed following Cu(II) treatment, all enzyme species were digested with endoproteinase Lys-C. The peptide mixtures obtained gave similar peptide maps when analyzed by LC-ESIMS. The fractions obtained were eventually characterized by Edman degradation for their peptide components. In all cases, peptides were identified within the protein sequence on the basis of their molecular mass and enzyme specificity. Furthermore, ESIMS analysis allowed the determination of the redox state of the cysteine residues present in each peptide. The peptides observed in each fraction are reported in Table I. As expected, the peptide maps obtained for the Cu(II)-treated species were almost identical to those of the native ones, with the differences being limited only to specific fractions.

In the case of untreated b-ALR2 and h-ALR2, the fraction eluting at 51.7 min contained components with molecular masses of 6,457.9 ± 0.9 and 6,418.3 ± 1.3 Da that were assigned to the bovine and human peptide-(263-315)-CAM_2, respectively. Edman degradation analysis confirmed the nature of these peptides, demonstrating the presence of a carboxamidomethyl group at both Cys^{298} and Cys^{303}. Minor components originating from hydrolysis at Lys^{282} (bovine) and Lys^{274} and Lys^{307} (human) were also observed. In all the other peptides detected, cysteines were present as carboxamidomethylated residues.

In the case of Cu(II)-treated b-ALR2 and h-ALR2, peptides-(263-315)-CAM_2 were present only in traces (Table I). However, the fraction eluting at 50.5 min presented main signals at mass

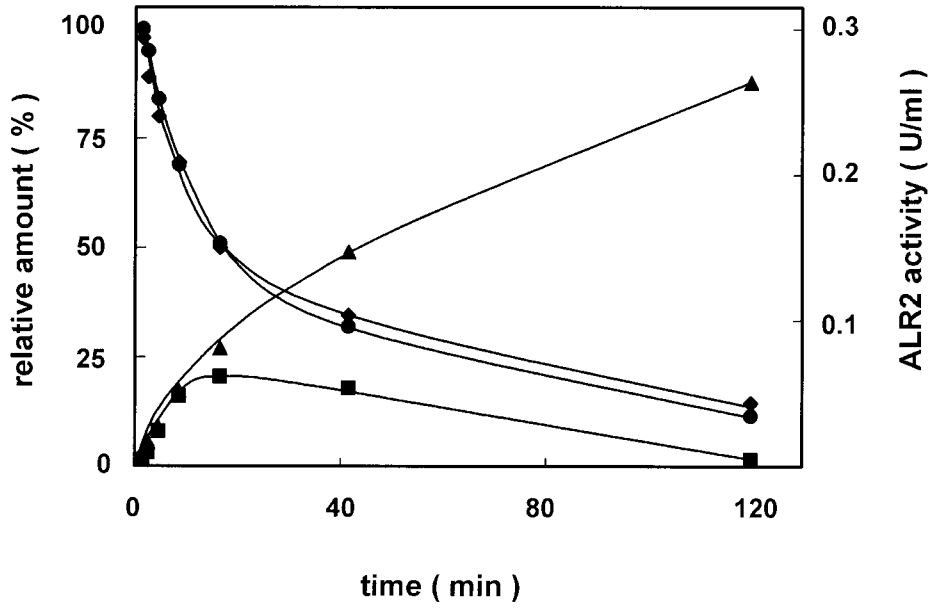

FIG. 4. **Time course of copper-induced disulfide generation on bovine lens ALR2.** b-ALR2 (7.5 μM) was incubated in the presence of 15 μM $CuCl_2$ at 25 °C. At different times the enzyme activity was measured (●). At the same times aliquots were withdrawn and the relative amounts of peptides carrying Cys^{80}, Cys^{298}, and Cys^{303} in different redox states were determined by LC-ESIMS analysis (see "Experimental Procedures"). The *symbols* refer to: ♦, all reduced Cys; ■, Cys^{80}-Cys^{303} disulfide; ▲, Cys^{298}-Cys^{303} disulfide.

6,341.7 ± 0.7 and 6,302.0 ± 1.0 Da that were associated with the bovine and human peptide-(263-315), respectively, where Cys^{298} and Cys^{303} were involved in an intramolecular disulfide bridge. Peptide sequencing of both fractions confirmed this hypothesis as demonstrated from the presence of the corresponding phenylthiohydantoin-derivative at the relative cycles. Also, in this case minor components originating from hydrolysis at Lys^{282} (bovine) and Lys^{274} and Lys^{307} (human) were observed.

The analysis of all the other fractions shown in Table I revealed, in all the enzyme species, that Cys^{44}, Cys^{80}, Cys^{92}, Cys^{186}, and Cys^{199} were in a fully carboxamidomethylated form. Therefore, these results clearly demonstrate that Cu(II) treatment induces in both bovine and human enzymes the same molecular rearrangement resulting in the specific S–S bridge pairing between Cys^{298} and Cys^{303}.

Following the alkylation reaction, ESIMS analysis of the h-C298S enzyme showed a single component at 36,049.4 ± 3.4 Da corresponding to a protein species containing six carboxamidomethyl groups (theoretical value 36,048.5 Da). Furthermore, the spectrum of the Cu(II)-treated h-C298S enzyme showed a main molecular species, whose molecular mass (35,932.9 ± 3.2 Da) was consistent with an ALR2 form containing an intramolecular disulfide bond and four carboxamidomethyl groups (theoretical value 35,932.5 Da), and traces of the fully reduced species. Peptide mapping experiments on the oxidized enzyme showed the occurrence of a clear signal at 7,365.2 ± 1.5 Da that was associated with peptides-(78-85) and -(263-315), containing Cys^{80} and Cys^{303} joined by a disulfide bridge (Table I). The nature of this species was confirmed by Edman degradation. A minor component originating from hydrolysis at Lys^{274} was also observed. Traces of peptides-(78-85)-CAM and -(263-315)-CAM were also present. These data demonstrated that in the case of h-C298S mutant, ALR2 oxidation can proceed through the alternative formation of a specific S–S bridge between Cys^{80} and Cys^{303}.

Time Course of Disulfide Generation—To definitively clarify the mechanism of Cu(II)-induced oxidation of b-ALR2, protein aliquots were taken at different times during copper treatment and quickly alkylated with iodoacetamide. Samples were digested as previously reported and a determination of the relative abundance of the peptides containing Cys^{80}, Cys^{298}, and Cys^{303} was calculated from the LC-ESIMS analysis by using the approach of Vinci *et al.* (27). The results reported in Fig. 4 clearly show that the ALR2 inactivation parallels Cys oxidation. The oxidation initially proceeds with the simultaneous formation of the disulfide Cys^{80}-Cys^{303} and Cys^{298}-Cys^{303}. However, the relative amount of the disulfide Cys^{80}-Cys^{303} decreases as reaction proceeds, whereas a concomitant increase in the disulfide Cys^{298}-Cys^{303} concentration can be observed. These results suggest that the disappearance of the disulfide Cys^{80}-Cys^{303} at long times of incubation can be tentatively associated with an intramolecular disulfide rearrangement that results only in the Cys^{298}-Cys^{303} species as already reported in Table I. As expected, a parallel decrease in the relative abundance of peptides containing these cysteines in the reduced form was observed.

Molecular Modeling of the Modified ALR2 Structures—To provide a description of the ALR2 structural changes associated with the Cu(II)-induced oxidation, thus generating the observed intramolecular disulfides, a molecular modeling approach was used. Simulations were performed to investigate both steps of the ALR2 modification by copper (*i.e.* the early formation of a noncovalent complex between copper and ALR2 and the subsequent formation of the disulfide bond).

Noncovalent Interactions between ALR2 and Copper—After two copper ions were positioned on the human holoenzyme as described under "Experimental Procedures," MM and MD in water were performed on the noncovalent complexes. MD simulations performed on the Cu(II)·Cys^{80}-Cys^{303} complex resulted in a substantial conformational rearrangement of the ALR2 C-terminal end, as graphically reported in Fig. 5*A*. Compared with the crystal structure, the C terminus carrying Cys^{303} moves significantly toward Cys^{80} thereby reducing the distance between the two S atoms from 6.9 Å to an average value of 3.7 Å. It is interesting to observe that the conformation of the segment carrying Cys^{80} is almost unaltered during MD, so this conformational change may be ascribed only to the C terminus. This finding is in agreement with the relative B-factor of the two regions, and finds precedents in the substantial conformational reorganization of segment 298–303 observed in the crystal structures of ALR2 complexed with the inhibitors Zopolrestat (50) and Tolrestat (51).

In the structures of this noncovalent complex, a stable complex between Cys^{80}, Cys^{303}, and the two copper ions was detected (Fig. 5*A, inset*). Each copper ion coordinates both cys-

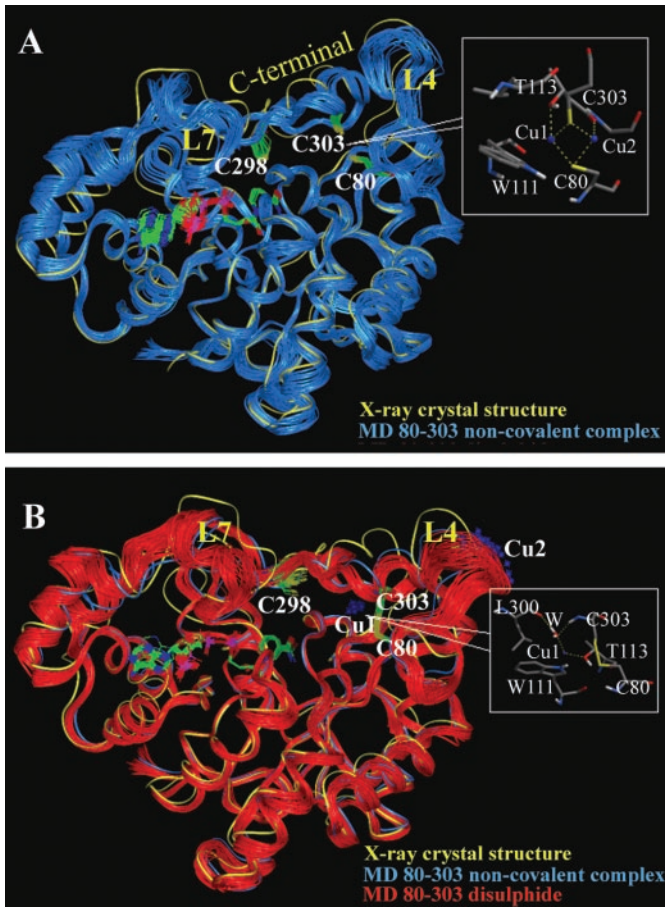

FIG. 5. **Molecular dynamics simulations of ALR2 interacting with copper at Cys^{80} and Cys^{303} residues.** MD at 27 °C was performed for copper-ALR2 noncovalent complex (*panel A*) and for the Cys^{80}-Cys^{303} disulfide-containing enzyme form (*panel B*). *Insets* in both panels show the magnification of the structure region in which the two copper ions were found. *Yellow line* refers to the structure of the holoenzyme from crystallographic data. Only the Cα trace of ALR2 is shown.

teines at an average distance of 2.3 Å. The formation of this noncovalent complex allows a substantial reduction of the distance between the two cysteines, with important consequences on the subsequent formation of the disulfide bond. Cys^{80} and Cys^{303} are close to each other and the nearby copper ions are able to undergo electron transfer in the following covalent steps.

In contrast to what was observed for Cys^{80} and Cys^{303}, MD simulations aimed at modeling the structures of noncovalent complexes between copper and Cys^{298} and Cys^{303} did not yield a significant shortening of the distance between these two cysteines. In fact, Cys^{298} and Cys^{303}, although able to coordinate the two copper ions, are separated by 12.3 Å in the crystal structure, and MD reduced their distance only to 11.3 ± 0.5 Å. A substantial rearrangement of the C-terminal segment would result in a shortened distance between these residues. Indeed, this rearrangement was already observed in the thermal rearrangement of Cys- and Cys-Gly mixed disulfide containing ALR2 (22). Modeling a process in which Cys^{298} and Cys^{303} approach each other as a result of copper binding would presumably require simulation times much longer than those used in the present work.

Disulfide Bond Formation—Starting from the structure of the noncovalent complex between copper and Cys^{80} and Cys^{303} (see above), a disulfide bond was imposed and the structure carrying the disulfide Cys^{80}-Cys^{303} was equilibrated with 800 ps of MD at 27 °C. The averaged structures collected during MD are graphically reported in Fig. 5*B*. Compared with the noncovalent structures described above, the C-terminal end moves even closer to the segment carrying Cys^{80} in the disulfide-containing structure. Cys^{298} is still far away from Cys^{80} and Cys^{303}. The loops L4 and L7, adjacent to the C-terminal end, exhibited the highest conformational flexibility during MD. Whereas one of the two copper ions that coordinate Cys^{80} and Cys^{303} in the noncovalent complex is now significantly distant from both cysteines and free to interact with water molecules and loop L4 (*Cu2* in Fig. 5*B*), the other copper ion (*Cu1*) remains completely embedded into the protein, interacting with Thr^{113}, Trp^{111}, Leu^{300}, and only one water molecule.

As the 300 ps MD simulation with the copper ions close to Cys^{298} and Cys^{303} failed to reach a noncovalent complex in which these cysteines were sufficiently close to conceive the formation of a disulfide, a starting structure with the Cys^{298}-Cys^{303} disulfide bond was modeled using Model er6, and then this structure was refined with 900 ps MD. Fig. 6 reports the averaged structures collected during MD. As expected, formation of the disulfide bond results in a significant refolding of the C-terminal segment. Three folded conformations of the C-terminal segment were sampled during MD, as it can be inferred from the clustering of conformations reported in the figure. In all cases, these conformations were significantly different from those observed in the crystal structure of ALR2, in which this segment is in an extended conformation. One of the two copper ions (Cu2) is, again, significantly distant from Cys^{298} and Cys^{303} and free to interact with water molecules and residues at the enzyme surface. The other (Cu1) remains embedded into the protein in a position similar to that already described for the Cys^{80}-Cys^{303} disulfide, even though solvent-exposed positions of this copper were also sampled during MD.

ALR2 Oxidation and Active Site—Tyr^{48} and His^{110} are two residues playing a fundamental role in the catalytic reduction of aldehydes by ALR2 (52, 53). A close inspection of the active site architecture reveals that Tyr^{48} and His^{110} are still properly located with respect to the C4-carbon of the nicotinamide of the cofactor after formation of the Cys^{80}-Cys^{303} and Cys^{298}-Cys^{303} disulfides. Fig. 7 reports a superimposition between these and a few nearby residues in the crystal structure of the holoenzyme and those in the MD disulfide-containing ALR2 structures. Whereas the phenol ring of Tyr^{48} superimposes very well, slight differences in the position of His^{110} have been observed. However, despite these differences, the average distance between the reactive C-4 of nicotinamide and the Nϵ-2 nitrogen of His^{110} was 5.6 ± 0.4 Å in the Cys^{80}-Cys^{303} disulfide structure and 5.4 ± 0.6 Å in the Cys^{298}-Cys^{303} disulfide structure. These compare well with the value of 5.1 Å in the ALR2 crystal structure. Similarly, the distances between C-4 of nicotinamide and the phenol oxygen of Tyr^{48} were 4.6 ± 0.4 and 4.4 ± 0.4 Å in the Cys^{80}-Cys^{303} and Cys^{298}-Cys^{303} MD structures, respectively. These also compare well with the distance of 4.5 Å in the crystal structure. In contrast, major differences were observed in the conformation of the side chain of Trp^{111}, which is more affected by the nearby disulfides Cys^{80}-Cys^{303} and Cys^{298}-Cys^{303} (Fig. 7, *A* and *B*, respectively). Conformational changes at Trp^{111} clearly depend on the C terminus rearrangement caused by the formation of the disulfides. Based on these results, the possibility that slight differences at His^{110}, coupled with marked differences at Trp^{111}, might result in an impaired kinetics cannot be ruled out. On the other hand, a small aldehyde like D-glyceraldehyde could still be manually docked into the structures of the modified active sites with the carbonyl of the aldehyde hydrogen bonded to Tyr^{48} and His^{110}, and without steric conflicts with the Trp^{111} side chain.

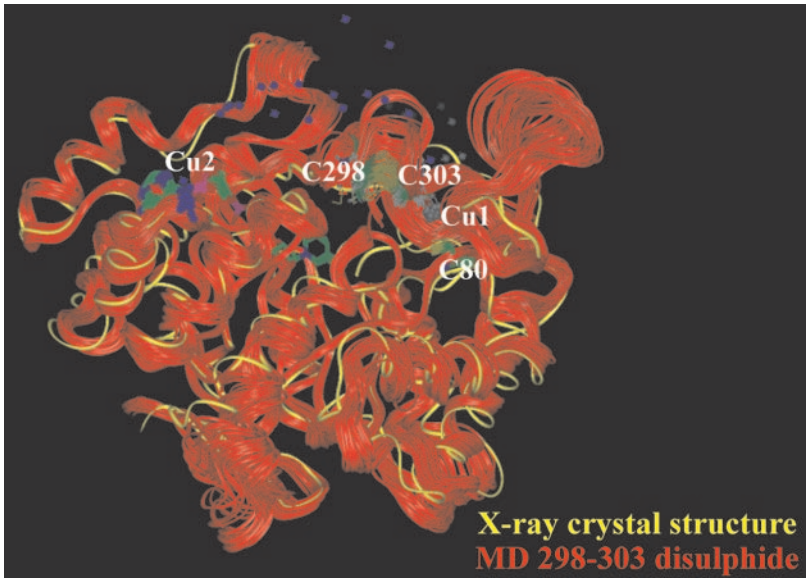

FIG. 6. **Molecular dynamics simulations of ALR2 interacting with copper containing the Cys^{298}-Cys^{303} disulfide.** MD at 27 °C was performed for Cys^{298}-Cys^{303} disulfide-containing ALR2 interacting with copper. *Yellow line* refers to the structure of the holoenzyme from crystallographic data. Only the Cα trace of ALR2 is shown.

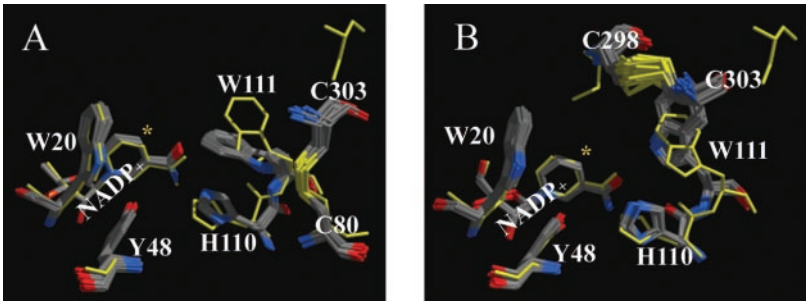

FIG. 7. **Active site comparison between Cys^{80}-Cys^{303} and Cys^{298}-Cys^{303} disulfide-containing ALR2.** Superimposition of Tyr^{48} and His^{110} and a few nearby residues at the active site in the crystal structure of the holoenzyme (in *yellow*) and those in the MD disulfide-containing ALR2 structures. *A*, Cys^{80}-Cys^{303}; and *B*, Cys^{298}-Cys^{303} disulfide-containing ALR2.

Enzyme Cofactor Binding following Copper-induced Inactivation—The possibility of a loss of the pyridine cofactor, following treatment of b-ALR2 with copper ion, was considered by evaluating the relative amount of NADP$^+$ bound to the copper-modified enzyme by CD spectroscopy. This evaluation was possible because the addition of DTT to the ALR2-cofactor complex generates a dichroic signal that peaks at 335 nm with an intensity proportional to the complex concentration (24). Fig. 8 shows the appearance of such a dichroic signal after addition of 5 mM DTT to copper-modified b-ALR2 previously dialyzed against S-buffer. A further increase of the signal intensity was observed when 10 μM NADP$^+$ was added to the enzyme sample. No further changes in the 280–370 nm spectral region were observed by further increases of the cofactor concentration to 20 μM (data not shown). The relative intensity of the CD signal at 335 nm of the DTT-treated, copper-modified ALR2 before and after addition of saturating NADP$^+$ accounted for a loss of ~60% of the pyridine cofactor from the Cu(II)-inactivated enzyme. This was evaluated by taking into account the dilution factor of 1.12 on the CD signal after addition of NADP$^+$. The same dilution factor was adopted to correct the protein contribution to the overall observed elongation.

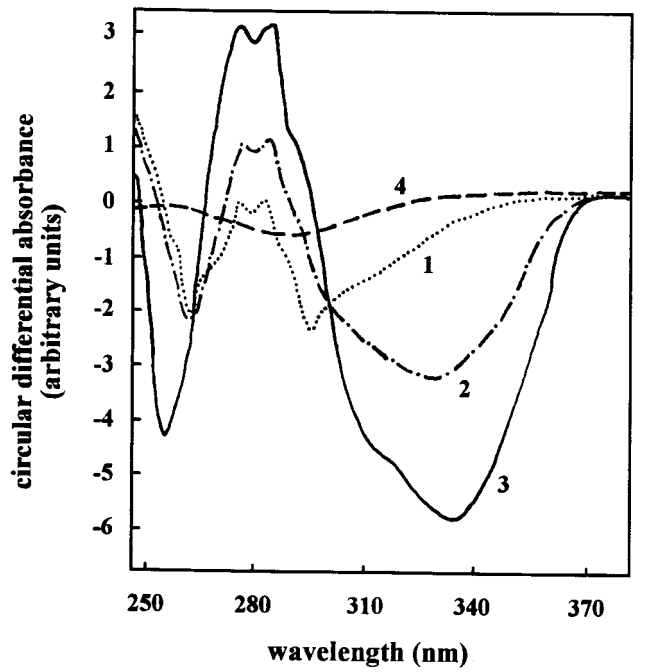

FIG. 8. **Circular dichroic spectra of Cu(II)-modified ALR2.** Spectra were obtained as described under "Experimental Procedures" with 10 μM Cu(II)-modified b-ALR2 in the following conditions: *curve 1*, S-buffer; *curve 2*, S-buffer supplemented with 5 mM DTT; *curve 3*, sample of curve 2 (1 ml) supplemented with 120 μl of 0.1 mM NADP$^+$ in 5 mM DTT. A superimposable spectrum was obtained when the sample of curve 2 was supplemented of 120 μl of 0.2 mM NADP$^+$ solution. No differences were observed in the 280–370 nm region of the S-buffer spectrum (*curve 4*) after addition of both 5 mM DTT and 10 μM NADP$^+$.

DISCUSSION

The human and rat recombinant forms of aldose reductase exhibited the same response to copper ion as the bovine lens enzyme. Both were inactivated by Cu(II) and ALR2 activity could be recovered by treating the inactive enzyme with DTT but not with EDTA or *o*-phenanthroline. Copper remained bound on the protein after inactivation. Whereas 1 eq of copper per enzyme mol is directly detectable as Cu(I), a total of 2 eq of copper per enzyme mol can be detected only after a 3-h treat-

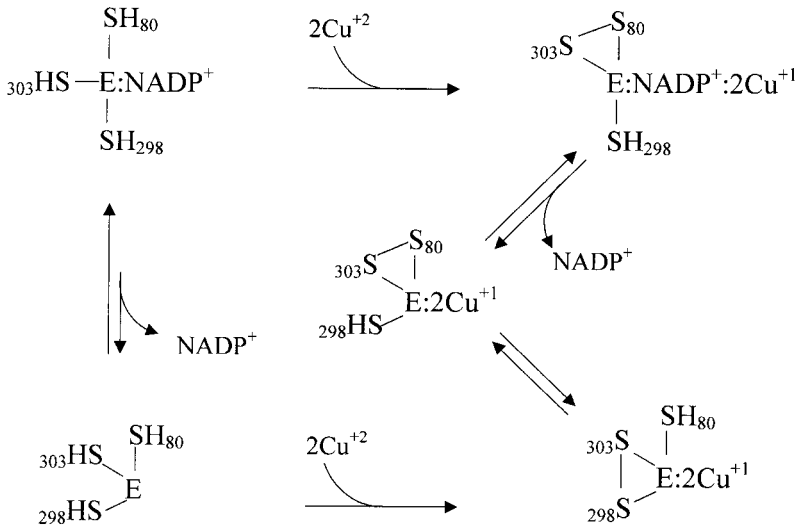

FIG. 9. **Model of copper induced oxidation of ALR2.**

ment at 37 °C of the inactive enzymes with either 3 mM DTT or 0.5 mM EDTA.

Cys^{303} is the only residue whose presence is essential for ALR2 inactivation. In fact, the h-C303S mutant reacts with copper quite differently from all other enzyme forms tested. When this mutant was incubated with copper in the presence of a stoichiometric amount of $NADP^+$, the enzyme activity remained essentially stable until the copper concentration was raised to values causing protein aggregation (17). Furthermore, when $NADP^+$ was not supplemented to the enzyme preparation, the copper treatment caused C303S mutant inactivation, which did not require DTT to be reversed, at variance with all other enzymes. In fact, in this case treatment with EDTA was sufficient to rescue the enzyme activity.

In this study, mass spectrometric analysis of Cu(II)-inactivated ALR2 of bovine and human, as well as, the mapping analysis of their peptides (Table I), revealed that the final product generated by copper treatment is an enzyme form carrying an intramolecular disulfide bond Cys^{298}-Cys^{303}. The involvement of Cys^{298} in the disulfide bridge explains the special reactivity of the oxidized ALR2 form with respect to monothiol compounds (Fig. 3). In fact, it appears clear that both GSH and 2-ME can disrupt the disulfide bond by targeting Cys^{298} and generate mixed disulfide enzyme forms either as intermediate species (*i.e.* reduction of oxidized b-ALR2 by GSH) and/or as end products (*i.e.* reduction of oxidized h-ALR2 and b-ALR2 by GSH and 2-ME). In this regard, the apparent lack of effectiveness of Cys in rescuing the enzyme activity, both in terms of recovery of the native enzyme form and of generation of the Cys-ALR2 mixed disulfide form, is in complete agreement with the rather low, unusual stability of Cys-ALR2 that was shown to rearrange at 37 °C back to the Cys^{298}-Cys^{303} disulfide-containing enzyme (22). The behavior of the h-C80S enzyme is in line with these results. However, the inactivation observed for the h-C298S enzyme following Cu(II) treatment (Fig. 2) and the presence of the intramolecular disulfide Cys^{80}-Cys^{303}, verified for the oxidized human mutant (Table I), raise the question on the mechanism underlying the modification processes. Indeed, whereas the kinetics of copper-induced inactivation of b-ALR2 is paralleled by the accumulation of the Cys^{298}-Cys^{303} disulfide, a transient formation of the Cys^{80}-Cys^{303} disulfide bond was also observed (Fig. 4). Thus the disulfide Cys^{80}-Cys^{303} can be generated not only in the Cys^{298} mutants, but also in the native enzyme. The transient appearance of the Cys^{80}-Cys^{303} disulfide enzyme and the progressive accumulation of the Cys^{298}-Cys^{303} disulfide enzyme (Fig. 4) necessarily imply the occurrence of an intramolecular rearrangement of the former enzyme form to the latter. Even though the results related to the h-C80S enzyme indicates the possible direct formation of the Cys^{298}-Cys^{303} disulfide, the exact oxidation pathway occurring on the native enzyme that gives rise to the end product of the copper-induced ALR2 oxidation remains an open question.

By inspection of the distances between the sulfur atoms of the cysteines in the crystal structure of the h-ALR2/$NADP^+$ holoenzyme (44) it turns out that while Cys^{298} and Cys^{303} are too far apart (12.3 Å) to be likely candidates for formation of a disulfide bond, Cys^{80} and Cys^{303} are relatively closer (6.9 Å). However, given that these cysteines are not close to a bonding distance, the formation of disulfide bridges must be accompanied by remarkable conformational changes in ALR2.

The structural changes allowing the generation of intramolecular disulfide bonds were investigated by a molecular modeling approach. Indeed, simulations were performed with the aim to investigate both steps of the ALR2 modification by copper (*i.e.* the early formation of a noncovalent complex between copper and ALR2 and the subsequent formation of the disulfide bond). Following the definition of the force field parameters for copper, a four-centered complex between Cys^{80}, Cys^{303}, and 2 copper ions could be envisaged for ALR2. During a molecular dynamics simulation of the copper-ALR2 noncovalent complex, the distance between the sulfur atoms of Cys^{80} and Cys^{303} dropped significantly (Fig. 5*A*). In this configuration each copper ion coordinates both cysteines. The closer distances between the two cysteines and between these residues and the copper ions were compatible with an electron transfer process that can proceed through the formation of the disulfide Cys^{80}-Cys^{303}. Molecular dynamics simulations of the ALR2 structure containing the disulfide were then performed to allow the conformational changes arising from the disulfide modification (Fig. 5*B*). One interesting observation was that, following the disulfide formation, the two copper ions appeared to interact to a lesser extent with the cysteine residues. In fact, whereas Cu2 significantly drifted apart from both residues (>10 Å) interacting with water molecules, Cu1, yet at non-coordinating distance from both the cysteines, appeared to remain completely embedded in the protein (Fig. 5*B*). This finding is in agreement with a previous experimental observation (17) that only one of the two copper ions bound to ALR2 can be detected by direct bathocuproinedisulfonic acid titration (Cu2 in our case). Moreover, the second copper ion (Cu1), which would be trapped by the enzyme upon formation of the disulfide, became detectable

only after the reduction of the enzyme (*i.e.* after removal of the disulfide bond) or after prolonged treatment of the modified ALR2 at 37 °C with EDTA.

Cys^{298} remained too far apart from other cysteines to participate in any disulfide bond. Any attempt to shorten its distance from Cys^{303} through the interaction with copper ions by MM and MD approaches using the crystal structure of the $NADP^+$·ALR2 complex failed. A substantial reduction of the distance between these residues could occur only after a refolding of the C-terminal segment. Conformational changes at the C terminus were previously observed in the crystal structures of ALR2 complexed with the inhibitors Zopolrestat (50) and Tolrestat (51), but in none of these structures were Cys^{298} and Cys^{303} closer than 11 Å. However, different experiments involving formation of mixed disulfides at 37 °C showed that thermal rearrangements of Cys- and Cys-Gly mixed disulfide containing ALR2 likely occurred by closer Cys^{298}-Cys^{303} interactions (22). Nevertheless, when the disulfide Cys^{303}-Cys^{298} was imposed, the two copper ions, initially positioned at a coordinating distance between Cys^{303} and Cys^{298}, drifted apart and became situated in a way similar to that described in the case of the Cys^{80}-Cys^{303} disulfide (Fig. 6).

One possible structural change that could allow Cys^{303} to move closer and interact either directly with Cys^{298} (as may be the case of the C80S enzyme) or with the disulfide bond Cys^{80}-Cys^{303}, may derive from the loss of the pyridine cofactor from the enzyme undergoing oxidation. A schematic representation of ALR2 modification induced by the copper ion is depicted in Fig. 9.

The loss of the cofactor should induce significant changes in the ALR2 conformation. In fact, the release of the cofactor, which is the rate-limiting step in the direction of aldehyde reduction, is known to be associated with remarkable conformational changes of loop 7 (54–57). Indeed, loop 7, which is adjacent to the Cys^{298}-Cys^{303} disulfide (Fig. 6), showed the highest conformational variability during MD, supporting the hypothesis that formation of the disulfide might affect the $NADP^+$ binding site and $NADP^+$ release. Such an event may also give the rationale for the lack of activity of the disulfide enzyme forms. In fact, from a closer view of the active site of the disulfide-carrying enzymes (Fig. 7), besides the conformational change observed at Trp^{111}, which may possibly affect enzyme activity, there are no apparent reasons for the oxidized holoenzyme to be inactive. Unfortunately, the high values of the kinetic constants of the reversible movement of loop 7 in the mechanism of action (*i.e.* 0.5 s^{-1}) (55), as well as the lack of useful crystal structure data on the ALR2 apoenzyme, made it very difficult to handle this problem by a molecular modeling approach. However, the involvement of the release of $NADP^+$ in the conformational rearrangements leading Cys^{303} to reach at bonding distance Cys^{298} is supported by the CD data. In fact, the analysis of CD spectra of the Cu(II)-modified b-ALR2 reveals that 60% of the $NADP^+$, usually firmly bound to native ALR2, was lost after copper treatment (Fig. 8).

In conclusion, the site-specific oxidative action of copper ion on ALR2 ends with one of the most easy to predict modifications (*i.e.* thiol oxidation to disulfides) that this metal ion is able to induce on target proteins. In this case, the evolution of the oxidative insult on the protein structure leads to an enzyme form that is inactive but still convertible to the active native enzyme and to an efficient copper sequestration. Whether such an apparent scavenging action exerted by ALR2 contributes to the control of oxidative insult is still a matter of investigation.

Acknowledgments—We are indebted to Dr. Nando Benimeo (Industrie Alimentari Carni, Castelvetro, Modena) for the kind supply of bovine lenses, and to Dr. Giovanni Sorlini and the veterinary staff of IN.AL.CA. for their valuable cooperation in bovine lens collection. We acknowledge Prof. Maurizio Zandomeneghi (Department of Chemistry, University of Pisa) for valuable expertise in the CD analysis. We thank Centro Interdipartimentale di Calcolo Elettronico, University of Modena, for access to the computers.

REFERENCES

1. Halliwell, B., and Gutteridge, M. C. (1984) *Biochem. J.* **219,** 1–14
2. Stückel, J., Wallace, A. C., Cohen, F. E., and Prusiner, S. B. (1998) *Biochemistry* **37,** 7185–7193
3. Linder, M. C., and Hazegh-Azam, M. (1996) *Am. J. Clin. Nutr.* **63**, 797S–811S
4. Yuan, D. S., Stearman, R., Dancis, A., Dunn, T., Beeler, T., and Klausner, R. D. (1995) *Proc. Natl. Acad. Sci. U. S. A.* **92,** 2632–2636
5. Petris, M. J., Mercer, J. F., Culvenor, J. G., Lockhart, P., Gleeson, P. A., and Camakaris, J. (1996) *EMBO J.* **15,** 6084–6095
6. Ogihara, H., Ogihara, T., Miki, M., Yasuda, H., and Mino, M. (1995) *Pediatr. Res.* **37,** 219–226
7. Tallis, G. A., Kitchener, M. I., and Thomas, A. C. (1990) *Clin. Chem.* **36,** 568–570
8. Harman, D. (1965) *J. Gerontol.* **20,** 151–153
9. Brewer, G. J., and Yuzbasiyan-Gurkan, V. (1992) *Medicine* **71,** 139–164
10. Lin, J. (1977) *Jpn. J. Ophthalmol.* **41,** 130–137
11. Ueda, J., Saito, N., and Ozawa, T. (1996) *Arch. Biochem. Biophys.* **325,** 65–76
12. Li, Y., Trush, M. A., and Yager, J. D. (1994) *Carcinogenesis* **15,** 1421–1427
13. Kobayashi, S., Ueda, K., Morita, J., Sakai, H., and Komano, T. (1988) *Biochim. Biophys. Acta* **949,** 143–147
14. Gutteridge, J. M., and Halliwell, B. (1982) *Biochem. Pharmacol.* **31,** 2801–2805
15. Aruoma, O. I., Halliwell, B., Gajewski, E., and Dizdaroglu, M. (1991) *Biochem. J.* **273,** 601–604
16. Garland, D. (1990) *Exp. Eye Res.* **50,** 677–682
17. Cecconi, I., Moroni, M., Vilardo, P. G., Dal Monte, M., Borella, P., Rastelli, G., Costantino, L., Garland, D., Carper, D., Petrash, J. M., Del Corso, A., and Mura, U. (1998) *Biochemistry* **37,** 14167–14174
18. Giannessi, M., Del Corso, A., Cappiello, M., Voltarelli, M., Marini, I., Barsacchi, D., Garland, D., Camici, M., and Mura, U. (1993) *Arch. Biochem. Biophys.* **300,** 423–429
19. Cappiello, M., Voltarelli, M., Cecconi, I., Vilardo, P. G., Dal Monte, M., Marini, I., Del Corso, A., Wilson, D. K., Quiocho, F. A., Petrash, J. M., and Mura, U. (1996) *J. Biol. Chem.* **271,** 33539–33544
20. Liu, S.-Q., Bhatnagar, A., and Srivastava, S. K. (1992) *Biochim. Biophys. Acta* **1120,** 329–366
21. Cappiello, M., Voltarelli, M., Giannessi, M., Cecconi, I., Camici, G., Manao, G., Del Corso, A., and Mura, U. (1994) *Exp. Eye Res.* **58,** 491–501
22. Vilardo, P. G., Scaloni, A., Amodeo, P., Barsotti, C., Cecconi, I., Cappiello, M., Lopez Mendez, B., Rullo, R., Dal Monte, M., Del Corso, A., and Mura, U. (2001) *Biochemistry* **40,** 11985–11994
23. Inagaki, K., Miwa, I., Yashiro, T., and Okuda, J. (1982) *Chem. Pharm. Bull.* **30,** 3244–3254
24. Del Corso, A., Barsacchi, D., Giannessi, M., Tozzi, M. G., Camici, M., Houben, J. L., Zandomeneghi, M., and Mura, U. (1990) *Arch. Biochem. Biophys.* **283,** 512–518
25. Petrash, J. M., Harter, T. M., Devine, C. S., Olins, P. O., Bhatnagar, A., Liu, S., and Srivastava, S. K. (1992) *J. Biol. Chem.* **267,** 24833–24840
26. Old, S. E., Sato, S., Kador, P. F., and Carper, D. A. (1990) *Proc. Natl. Acad. Sci. U. S. A.* **87,** 4942–4945
27. Vinci, F., Ruoppolo, M., Pucci, P., Freedman, R. B., and Marino, G. (2000) *Protein Sci.* **9,** 525–535
28. Bradford, M. M. (1976) *Anal. Biochem.* **72,** 248–254
29. Case, D. A., Pearlman, D. A., Caldwell, J. W., Cheathan, T. E., III, Ross, W. S., Simmerling, C. L., Darden, T. A., Merz, K. M., Stanton, R. V., Cheng, A. L., Vincent, J. J., Crowley, M., Tsui, V., Radmer, R. J., Duan, Y., Pitera, J., Massova, I., Seibel, G. L., Singh, U. C., Weiner, P. K., and Kollman, P. A. (1999) *AMBER6*, University of California, San Francisco, CA
30. Cornell, W. D., Cieplak, P., Bayly, C. I., Gould, I. R., Merz, K. M., Ferguson, D. M., Spellmeyer, D. C., Fox, T., Caldwell, J. W., and Kollman, P. A. (1995) *J. Am. Chem. Soc.* **117,** 5179–5197
31. Ferrin, T. E., Huang, C. C., Jarvis, L. E., and Langridge, L. (1988) *J. Mol. Graph.* **6,** 13–27
32. Hay, B. P. (1993) *Coord. Chem. Rev.* **126,** 177–236
33. Weast, R. C., Astle, M. J., Beyer, W. H. (1985–1986) *Handbook of Chemistry and Physics*, 66th Edition, Section F-164, CRC Press, Boca Raton, FL
34. Guss, J. M., Bartunik, H. D., and Freeman, H. C. (1992) *Acta Cryst. Sect. B* **48,** 790–811
35. Ryde, U., Ollson, M. H. M., Pierloot, K., and Roos, B. O. (1996) *J. Mol. Biol.* **261,** 586–596
36. Pierloot, K., De Kerpel, J. O. A., Ryde, U., and Roos, B. O. (1997) *J. Am. Chem. Soc.* **119,** 218–226
37. Frisch, M. J., Trucks, G. W., Schlegel, H. B., Gill, M. W., Johnson, B. G., Robb, M. A., Cheeseman, J. R., Keith, T., Petersson, G. A., Montgomery, J. A., Raghavachari, K., Al-Laham, M. A., Zakrzewski, V. G., and Ortiz, J. V. (1995) *Gaussian94,* Revision D, Gaussian, Inc., Pittsburgh, PA
38. Bayly, C. I., Cieplak, P., Cornell, W. D., and Kollman, P. A. (1993) *J. Phys. Chem.* **97,** 10269–10277
39. Cieplak, P., Bayly, C. I., Cornell, W. D., and Kollman, P. A. (1995) *J. Comput. Chem.* **16,** 1357–1377
40. Åqvist, J. (1990) *J. Phys. Chem.* **94,** 8021–8024
41. Jorgensen, W. L., Buckner, J. K., Huston, S. E., and Rossky, P. J. (1987) *J. Am. Chem. Soc.* **109,** 1891–1899
42. Jorgensen, W. L., Chandrasekhar, J., Madura, J. D., Impey, R. W., and Klein, M. L. (1983) *J. Chem. Phys.* **79,** 926–935

43. van Gusteren, W. F., and Berendsen, H. J. C. (1977) *Mol. Phys.* **34,** 1311–1327
44. Wilson, D. K., Bohren, K. M., Gabbay, K. H., and Quiocho, F. H. (1992) *Science* **257,** 81–84
45. Sali, A., and Blundell, T. L. (1993) *J. Mol. Biol.* **234,** 779–815
46. Laskowski, R. A., McArthur, M. W., Moss, D. S., and Thornton, J. M. (1993) *J. Appl. Cryst.* **26,** 283–291
47. Schade, S. Z., Sherrell, L. E., Williams, T. R., Kezdy, F. J., Heinrikson, R. L., Grimshaw, C. E., and Doughty, C. C. (1990) *J. Biol. Chem.* **265,** 3628–3635
48. Bohren, K. M., and Gabbay, K. H. (1993) in *Enzymology and Molecular Biology of Carbonyl Metabolism* (Weiner, H., ed) Vol. 4, pp. 267–277, Plenum Press, New York
49. Cappiello, M., Vilardo, P. G., Cecconi, I., Leverenz, V., Giblin, F. J., Del Corso, A., and Mura, U. (1995) *Biochem. Biophys. Res. Commun.* **207,** 775–782
50. Wilson, D. K., Tarle, I., Petrash, J. M., and Quiocho, F. A. (1993) *Proc. Natl. Acad. Sci. U. S. A.* **90,** 9847–9851
51. Urzhumtsev, A., Tete-Favier, F., Mitschler, A., Barbanton, J., Barth, P., Urzhumtseva, L., Biellmann, J. F., Podjarni, A. D., and Moras, D. (1997) *Structure* **5,** 601–612
52. Bohren, K. M., Grimshaw, C. E., Lai, C.-J., Harrison, D. H., Ringe, D., Petsko, G. A., and Gabbay, K. H. (1994) *Biochemistry* **33,** 2021–2032
53. Tarle, I., Borhani, D. W., Wilson, D. K., Quiocho, F. A., and Petrash, J. M. (1993) *J. Biol. Chem.* **268,** 25687–25693
54. Grimshaw, C. E., Shabbaz, M., and Putney, G. C. (1990) *Biochemistry* **29,** 9947–9955
55. Grimshaw, C. E., Bohren, K. M., Lai, C.-J., and Gabbay, K. H. (1995) *Biochemistry* **34,** 14356–14365
56. Grimshaw, C. E., Bohren, K. M., Lai, C.-J., and Gabbay, K. H. (1995) *Biochemistry* **34,** 14366–14373
57. Kubiseski, T. J., Hindman, D. J., Morjana, N. A., and Flynn, T. G. (1992) *J. Biol. Chem.* **267,** 6510–6517